Inorg. Chem. **2004**, *43*, 1287−1293

Preparation of Acentric Porous Coordination Frameworks from an Interpenetrated Diamondoid Array through Anion-Exchange Procedures: Crystal Structures and Properties

Miao Du, Ya-Mei Guo, Shen-Tan Chen, and Xian-He Bu*

Department of Chemistry, Nankai University, Tianjin 300071, P. R. China

Stuart R. Batten

School of Chemistry, P.O. Box 23, Monash University, Clayton, Victoria 3800, Australia

Joan Ribas

Departament de Química Inorgànica, Universitat de Barcelona, Diagonal 647, 08028-Barcelona, Spain

Susumu Kitagawa

Department of Synthetic Chemistry and Biological Chemistry, Graduate School of Engineering, Kyoto University, Kyoto 606-8501, Japan

Received September 25, 2003

The formation, crystal structures, and properties of a series of three-dimensional (3-D) Cu^{II} coordination polymers, $\{[Cu(\mathbf{L})_2(H_2O)_2](PF_6)_2(H_2O)_{1.25}\}_n$ (**1**), $\{[Cu\mathbf{L}(N_3)_2](H_2O)_{1.5}\}_n$ (**2**), and $\{[Cu\mathbf{L}(H_2O)(SO_4)](H_2O)_2\}_n$ (**3**), with an angular bridging ligand 2,5-bis(4-pyridyl)-1,3,4-oxadiazole (**L**) are reported. Complex **1** crystallizes in the tetragonal $I4_1/a$ space group ($a = b = 13.462(2)$ Å, $c = 46.47(1)$ Å, $Z = 8$), complex **2** in the orthorhombic $Pna2_1$ space group ($a = 6.379(2)$ Å, $b = 10.060(3)$ Å, $c = 27.232(9)$ Å, $Z = 4$), and complex **3** in the orthorhombic $P2_12_12_1$ space group ($a = 5.510(2)$ Å, $b = 10.576(4)$ Å, $c = 28.34(1)$ Å, $Z = 4$). Different polymeric frameworks are obtained by only varying the counterions. These include the 2-fold interpenetrated diamondoid structure of **1**, the acentric α-Po network of **2**, and the chiral open framework of **3** with $(6^3).(6^9.8)$ topology. The interesting anion-exchange, porous, and magnetic properties of these coordination supramolecules have been investigated in detail.

Introduction

The design and synthesis of noncentrosymmetric solids, especially chiral metal−organic coordination architectures, is one of the most fascinating and challenging problems as such systems have potential applications in many fields, such as nonlinear optical (NLO) materials, asymmetric catalysis, and stereoselective recognition or inclusion.[1] One of the most effective methods for achieving a chiral three-dimensional (3-D) structure within a given crystal is to spontaneously resolve the 1-D polymeric helicates through weak intermolecular attractive forces such as C−H···π or H-bonding interactions.[2,3] However, 3-D metal−organic chiral coordination frameworks constructed through stronger metal−ligand bonds are still quite rare and completely reliant on spontane-

* To whom correspondence should be addressed. E-mail: buxh@nankai.edu.cn. Fax: +86-22-23502458. Tel: +86-22-23502809.

(1) For example: (a) Lehn, J.-M. *Supramolecular Chemistry−Concept and Perspectives*; VCH: Weinheim, Germany, 1997. (b) Abrahams, B. F.; Jackson, P. A.; Robson, R. *Angew. Chem., Int. Ed.* **1998**, *37*, 2656−2659. (c) Seo, J. S.; Whang, D.; Lee, H.; Jun, S. I.; Oh, J.; Jeon, Y. J.; Kim, K. *Nature* **2000**, *404*, 982−986. (d) Evans, O. R.; Ngo, H. L.; Lin, W. *J. Am. Chem. Soc.* **2001**, *123*, 10395−10396. (e) Maggard, P. A.; Stern, C. L.; Poeppelmeier, K. R. *J. Am. Chem. Soc.* **2001**, *123*, 7742−7743. (f) Xiong, R.-G.; You, X.-Z.; Abrahams, B. F.; Xue, Z.; Che, C.-M. *Angew. Chem., Int. Ed.* **2001**, *40*, 4422−4425. (g) Kondo, M.; Miyazawa, M.; Irie, Y.; Shinagawa, R.; Horiba, T.; Nakamura, A.; Naito, T.; Maeda, K.; Utsuno, S.; Uchida, F. *Chem. Commun.* **2002**, 2156−2157.

(2) Biradha, K.; Seward, C.; Zaworotko, M. J. *Angew. Chem., Int. Ed.* **1999**, *38*, 492−495.

10.1021/ic0351242 CCC: $27.50
Published on Web 02/03/2004

Chart 1

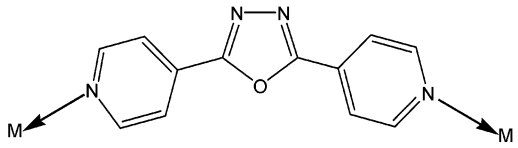

ous self-assembly in most cases.[4] It should be noted that the preparation of a series of acentric or chiral 2-D or 3-D coordination polymers using unsymmetrical organic linking groups together with their second-order NLO properties have been reported recently.[5] Significantly, these chiral architectures are generated from simple achiral building blocks and metal centers without any chiral auxiliary.

Recently, an angular dipyridyl bridging ligand, 2,5-bis-(4-pyridyl)-1,3,4-oxadiazole (**L**, Chart 1),[6a] and its 3,3′-N-donor analog[6e] have attracted our attention with regard to structural control of discrete or divergent supramolecular architectures upon metal complexation under appropriate conditions.[6] The effects of anions on the self-assembly processes of Cu^{II} and both building blocks were investigated,[6a,e] and a unique 2-fold interpenetrating diamondoid network with **L**, $\{[Cu(\mathbf{L})_2(H_2O)_2](ClO_4)(OH)(H_2O)_{2.5}\}_n$ (**1a**), which is dependent on the choice of anion, has been obtained.[6a] This structure consists of two topologically equivalent but enantiomeric interpenetrating networks, which makes it of further interest with regards to asymmetric induction (such as the bridging anions in this study) of supramolecular chirality in network assembly.[4] Thus, in this contribution, we will report a synthetic approach toward two unique acentric metal−organic open frameworks $\{[Cu\mathbf{L}(N_3)_2](H_2O)_{1.5}\}_n$ (**2**) and $\{[Cu\mathbf{L}(H_2O)(SO_4)](H_2O)_2\}_n$ (**3**) with different topologies through anion-exchange procedures from the precursor **1a** or its isostructural compound $\{[Cu(\mathbf{L})_2(H_2O)_2](PF_6)_2(H_2O)_{1.25}\}_n$ (**1**).

Experimental Section

Materials and General Methods. With the exception of the bridging ligand 2,5-bis(4-pyridyl)-1,3,4-oxadiazole (**L**), which was synthesized according to reported literature procedure,[7] all of the starting materials and solvents were obtained commercially and used as received. Fourier transform (FT) IR spectra (KBr pellets) were taken on a FT-IR 170SX (Nicolet) spectrometer. Carbon, hydrogen, and nitrogen analyses were performed on a Perkin-Elmer 240C analyzer. Thermogravimetric analysis (TGA) experiment was carried out on a Dupont thermal analyzer from room temperature to 800 °C under nitrogen atmosphere at a heating rate of 10 °C/min. X-ray powder diffraction (XRPD) data were recorded on a Rigaku RU200 diffractometer at 60 kV, 300 mA for Cu Kα radiation ($\lambda = 1.5406$ Å), with a scan speed of 2 deg/min and a step size of 0.02° in 2θ. The calculated XRPD pattern was produced using the SHELXTL-XPOW program and single-crystal diffraction data.

Magnetic Studies. The variable-temperature magnetic susceptibilities were measured in "Servei de Magnetoquímica (Universitat de Barcelona)" on polycrystalline samples (ca. 30 mg) with a Quantum Design MPMS SQUID susceptometer operating at a magnetic field of 0.1 T between 2 and 300 K. The diamagnetic corrections were evaluated from Pascal's constants for all the constituent atoms. Magnetization measurements were carried out at low temperature (2 K) in the 0−5 T range.

Syntheses of Cu^{II} Complexes. $\{[Cu(L)_2(H_2O)_2](PF_6)_2(H_2O)_{1.25}\}_n$ (1). To the microcrystalline sample of compound $\{[Cu(\mathbf{L})_2(H_2O)_2](ClO_4)(OH)(H_2O)_{2.5}\}_n$ (**1a**) (177 mg, 0.25 mmol) was slowly added an excess of $NaPF_6$ (143 mg, 0.85 mmol) in aqueous solution (60 mL) with vigorous mixing for 30 min, and a small quantity of light-blue powders of **1** was obtained, which were dissolved in additional water (20 mL). The reaction mixture was filtered and left to stand at room temperature. Well-shaped prismatic blue single crystals suitable for X-ray analysis were obtained after several weeks by slow evaporation of the solvent. Yield: 97 mg (45%). Anal. Calcd for $\{[Cu(\mathbf{L})_2(H_2O)_2](PF_6)_2(H_2O)_{1.25}\}_n$: C, 33.50; H, 2.64; N, 13.02. Found: C, 33.11; H, 3.09; N, 13.14. IR (cm^{-1}): 3441 b, 1621 s, 1570 m, 1542 m, 1488 m, 1430 s, 1384 vs, 1277 m, 1220 m, 1124 w, 1061 m, 1023 m, 1007 w, 969 w, 843 vs, 748 m, 733 m, 710 s, 561 m.

$\{[CuL(N_3)_2](H_2O)_{1.5}\}_n$ (2). To the microcrystalline sample of complex **1** (103 mg, 0.12 mmol) was slowly added an aqueous solution (40 mL) of NaN_3 (18 mg, 0.27 mmol) with stirring for 15 min, and green powders of **2** precipitated immediately, which were filtered off, washed with methanol/water, and dried under vacumm. Yield: 41 mg (85%). Deep green crystals of **2** suitable for X-ray determination were obtained by slow diffusion in an H-shaped tube of aqueous solutions of NaN_3 on one arm and complex **1** on the other one. Anal. Calcd for $\{[Cu\mathbf{L}(N_3)_2](H_2O)_{1.5}\}_n$: C, 36.13; H, 2.78; N, 35.10. Found: C, 35.89; H, 2.97; N, 35.02. IR (cm^{-1}): 3420 b, 2049 vs, 1620 s, 1567 m, 1541 m, 1478 m, 1426 s, 1346 m, 1295 w, 1277 w, 1236 w, 1121 w, 1092 w, 1057 m, 1026 m, 999 w, 971 w, 844 s, 748 w, 731 m, 714 s, 706 m, 656 w, 602 w, 612 m.

$\{[CuL(H_2O)(SO_4)](H_2O)_2\}_n$ (3). To the microcrystalline sample of complex **1** (260 mg, 0.30 mmol) was slowly added an aqueous solution (80 mL) of Na_2SO_4 (50 mg, 0.35 mmol) with stirring, and light blue-green powders of **3** precipitated soon, which were filtered off, washed with methanol/water, and dried under vacumm. The filtrate was allowed to stand at room temperature, and light green block crystals suitable for X-ray determination were collected after several weeks by slow evaporation of the solvent. Yield: 90 mg (68%). Anal. Calcd for $\{[Cu\mathbf{L}(H_2O)(SO_4)](H_2O)_2\}_n$: C, 32.91; H, 3.22; N, 12.79. Found: C, 32.77; H, 3.41; N, 12.86. IR (cm^{-1}): 3416 b, 1625 s, 1573 m, 1542 m, 1485 s, 1434 s, 1336 m, 1289 m, 1222 s, 1184 s, 1126 s, 1098 s, 1062 s, 1027 vs, 990 s, 959 s, 873 m, 848 s, 748 m, 736 m, 709 s, 661 m, 607 s, 542 m, 514 s.

Complexes **2** and **3** can also be obtained according to the same synthetic procedures as above except using complex **1a** instead of **1** as the starting material.

(3) Ezuhara, T.; Endo, K.; Aoyama, Y. *J. Am. Chem. Soc.* **1999**, *121*, 3279−3283.

(4) (a) Carlucci, L.; Ciani, G.; Macchi, P.; Proserpio, D. M. *Chem. Commun.* **1998**, 1837−1838. (b) Blake, A. J.; Champness, N. R.; Cooke, P. A.; Nicolson, J. E. B. *Chem. Commun.* **2000**, 665−666. (c) Sasa, M.; Tanaka, K.; Bu, X. H.; Shiro, M.; Shionoya, M. *J. Am. Chem. Soc.* **2001**, *123*, 10750−10751.

(5) Evans, O. R.; Lin, W. *Acc. Chem. Res.* **2002**, *35*, 511−522 and references therein.

(6) (a) Du, M.; Bu, X. H.; Guo, Y. M.; Liu, H.; Batten, S. R.; Ribas, J.; Mak, T. C. W. *Inorg. Chem.* **2002**, *41*, 4904−4908. (b) Du, M.; Chen, S. T.; Bu, X. H. *Cryst. Growth Des.* **2002**, *2*, 625−629. (c) Du, M.; Liu, H.; Bu, X. H. *J. Chem. Crystallogr.* **2002**, *32*, 57−61. (d) Fang, Y. Y.; Liu, H.; Du, M.; Guo, Y. M.; Bu, X. H. *J. Mol. Struct.* **2002**, *608*, 229−233. (e) Du, M.; Bu, X. H.; Huang, Z.; Chen, S. T.; Guo, Y. M.; Diaz, C.; Ribas, J. *Inorg. Chem.* **2003**, *42*, 552−559. (f) Dong, Y. B.; Ma, J, P.; Huang, R. Q.; Liang, F. Z.; Smith, M. D. *J. Chem. Soc., Dalton Trans.* **2003**, 1472−1479. (g) Dong, Y. B.; Cheng J. Y.; Wang H. Y.; Huang R. Q.; Tang B.; Smith M. D.; Loye H.-C. *Chem. Mater.* **2003**, *15*, 2593−2604 and references therein.

(7) Bentiss, F.; Lagrenee, M. *J. Heterocycl. Chem.* **1999**, *36*, 1029−1032.

Table 1. Crystal Data and Structure Refinement Parameters for Complexes **1**−**3**

	1	**2**	**3**
chem formula	$C_{24}H_{22.5}CuF_{12}N_8O_{5.25}P_2$	$C_{12}H_{11}CuN_{10}O_{2.5}$	$C_{12}H_{14}CuN_4O_8S$
fw	860.48	398.85	437.87
cryst syst	tetragonal	orthorhombic	orthorhombic
space group	$I4_1/a$	$Pna2_1$	$P2_12_12_1$
a (Å)	13.4623(16)	6.379(2)	5.5102(19)
b (Å)	13.4623(16)	10.060(3)	10.576(4)
c (Å)	46.472(12)	27.232(9)	28.344(10)
V (Å^3)	8422(3)	1747.3(10)	1651.9(10)
Z	8	4	4
ρ_{calcd} (g/cm^3)	1.357	1.516	1.501
$F(000)$	3452	808	892
μ (cm^{-1})	6.87	12.82	17.61
measd reflcns	15450	6616	6724
indpndnt reflcns	3372	2547	2875
R_{int}	0.1286	0.1229	0.0598
S	0.992	1.007	0.995
R[a]	0.0738	0.0489	0.0406
R_w[b]	0.1698	0.1229	0.0703

[a] $R = \sum||F_o| - |F_c||/\sum|F_o|$. [b] $R_w = [\sum[w(F_o^2 - F_c^2)^2]/\sum w(F_o^2)^2]^{1/2}$.

Caution! *Azido and perchlorate complexes of metal ions in the presence of organic ligands are potentially explosive. Only a small amount of material should be prepared, and it should be handled with care.*

X-ray Data Collection and Structure Determinations. X-ray single-crystal diffraction data for complexes **1**−**3** were collected on a Bruker Smart 1000 CCD area-detector diffractometer at 293(2) K with Mo Kα radiation ($\lambda = 0.71073$ Å) by the ω scan mode. The program SAINT[8] was used for integration of the diffraction profiles. All the structures were solved by direct methods using the SHELXS program of the SHELXTL package and refined by full-matrix least-squares methods with SHELXL (semiempirical absorption corrections were applied using SADABS program).[9] Cu^{II} atoms in each complex were located from the *E*-maps, and other non-hydrogen atoms were located in successive difference Fourier syntheses and refined with anisotropic thermal parameters on F^2. The hydrogen atoms of **L** were generated theoretically onto the specific atoms and refined isotropically with fixed thermal factors. The flack parameters for complexes **2** and **3** were refined to 0.00(1) and 0.03(2), respectively, indicating the correct absolute configuration. The structure of **3** was also reported elsewhere very recently.[6f] Further details for structural analysis are summarized in Table 1.

Results and Discussion

Synthesis and General Characterization. Complex **1** was obtained by reacting compound **1a** with excess $NaPF_6$ in aqueous solution, and this procedure is reversible. The acentric or chiral 3-D coordination polymers **2** and **3** can be obtained either from complex **1a** or **1** and NaN_3 or Na_2SO_4 through anion-exchange procedures. The anion-exchange reactions essentially involved placing crystals of compound **1** or **1a** in an aqueous solution including the appropriate anion. Given the change in Cu:**L** ratio between the precursors **1** or **1a** and the products **2** or **3**, and the gross structural changes, it is likely that the reaction occurs via dissolution of the precursor before (or simultaneously with) crystallization of the final product (complexes **2** and **3** are less soluble than **1**). This is also supported by an excellent recent study on anion exchange in Ag/4,4′-bipyridine coordination polymers.[10] Complexes **1** and **3** could also be directly prepared in water by simply stirring the correct stoichiometric mixture of suitable $Cu(PF_6)_2$ or $CuSO_4$ salts and **L** (see Scheme 1).

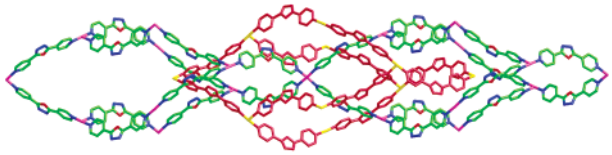

Figure 1. Interpenetrating adamantane cages from the two separate networks in **1**.

Scheme 1. Synthetic Strategies for Complexes **1**−**3**

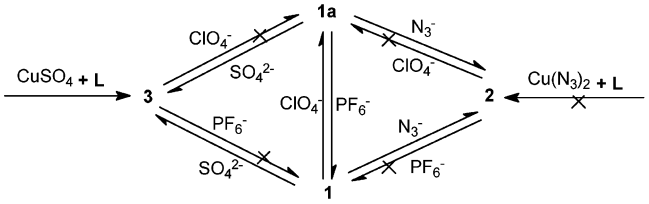

In the IR spectra of complexes **1**−**3**, the broad band centered at ca. 3400 cm^{-1} indicates the O−H stretching of the aqua molecules. The absorption bands resulting from the skeletal vibrations of aromatic rings of **L** for all three complexes appear in 1400−1600 cm^{-1} region. For **1**, the characteristic band (very strong) of the PF_6^- anions appears at 843 cm^{-1}. The IR spectra for **2** display the characteristic bands of the N_3^- anions at 2049 cm^{-1} (ν_{as}) and 1236 cm^{-1} (ν_s). For **3**, the bands of SO_4^{2-} groups appear at 1027−1126, 959, and 661 cm^{-1}, indicating the monodendate or tridendate coordinated mode (C_{3v} symmetry) with Cu^{II}. All these spectral features are consistent with the crystal structures as described below.

X-ray Single-Crystal Structures of Complexes 1−3. $\{[Cu(L)_2(H_2O)_2](PF_6)_2(H_2O)_{1.25}\}_n$ (1). A single-crystal X-ray study of complex **1** reveals that its structure is isomorphous with complex **1a**, exhibiting a 2-fold interpenetrated diamondoid network[6a,11] as shown in Figure 1. The Cu^{II} center, lying on a crystallographic 2-fold axis, coordinates to four trans **L** ligands and two axial water ligands (see Figure S1, Supporting Information) and displays an octahedral coordination geometry with considerable Jahn−Teller distortion (Table 2). Although the bridging ligands **L** coordinate to the Cu^{II} center in a square-planar form, the bent geometry of them allows the Cu^{II} center to act effectively as distorted tetrahedral nodes. The ligands connect the Cu^{II} atoms into 3-D diamond-like networks, and due to the spacious nature of the net, there are in fact a pair of *identical complementary* networks, interpenetrating to generate this structure (Figure 1). Each single net can be described in the chiral space group $I4_1$ (*the chirality may arise from the asymmetric nature of*

(8) Bruker AXS, *SAINT Software Reference Manual*; Siemens: Madison, WI, 1998.
(9) Sheldrick, G. M. *SHELXTL NT Version 5.1. Program for Solution and Refinement of Crystal Structures*: University of Göttingen: Göttingen, Germany, 1997.
(10) Khlobystov, A. N.; Champness, N. R.; Roberts, C. J.; Tendler, S. J. B.; Thompson, C.; Schröder, M. *CrystEngComm* **2002**, *4*, 426−431.
(11) (a) Hirsch, K. A.; Wilson, S. R.; Moore, J. S. *Chem.*−*Eur. J.* **1997**, *3*, 765−771. (b) Blake, A. J.; Champness, N. R.; Hubberstey, P.; Li, W.-S.; Withersby, M. A.; Schröder, M. *Coord. Chem. Rev.* **1999**, *183*, 117−138.

Table 2. Selected Bond Distances (Å) and Angles (deg) for Complex **1**[a]

Cu(1)−N(1)	2.047(5)	Cu(1)−N(4)	2.048(4)
Cu(1)−O(2A)	2.465(5)		
N(4B)−Cu(1)−N(4C)	89.8(3)	N(4C)−Cu(1)−N(1)	175.4(2)
N(4B)−Cu(1)−N(1)	91.2(2)	N(1A)−Cu(1)−N(1)	86.6(3)
O(2)−Cu(1)−O(2B)	175.1(2)	O(2)−Cu(1)−N(1)	89.2(3)
O(2)−Cu(1)−N(1A)	94.3(3)	O(2)−Cu(1)−N(4)	88.0(3)
O(2)−Cu(1)−N(1A)	88.1(3)		

[a] Symmetry operations: (A) $-x+1, -y+1/2, z$; (B) $y+1/4, -x+1/4, z+1/4$; (C) $-y+3/4, x+1/4, z+1/4$.

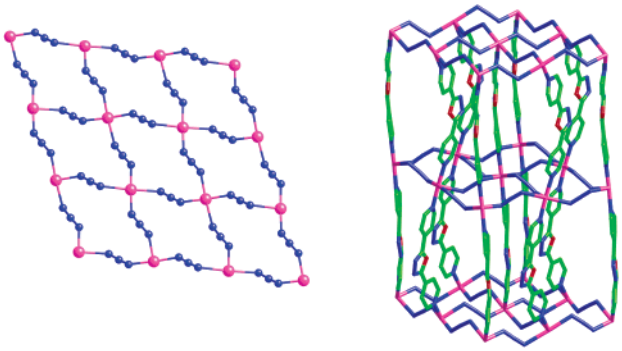

Figure 2. Structure of compound **2**, showing (left) the bridging of the metal ions by $\mu_{1,3}$ bridging azide ligands into a (4,4) sheet and (right) the bridging of these sheets by **L** into a single α-Po related network. Copper atoms are purple, nitrogens blue, oxygens red, and carbons green.

L), and the pair of opposite chirality produces the final observed $I4_1/a$ crystals. An analysis of the voids[12] shows ca. 14% of void even if calculated with the water molecules, and after the removal of these solvents, the void adds up to 24% and a set of mutually perpendicular cylindrical channels running along the [100] and [010] directions are visible (see Figure S2).

{[CuL(N$_3$)$_2$](H$_2$O)$_{1.5}$}$_n$ (2) and {[CuL(H$_2$O)(SO$_4$)](H$_2$O)$_2$}$_n$ (3). The crystal structures of complexes **2** and **3** both consist of linear [−Cu**L**−]$_n$ infinite chains which are linked by the 2-D layers of anions bridging between the metal centers to give 3-D networks. The two networks differ, however, in the topology of the metal−anion layers. In compound **2**, Cu^{II} centers are bridged by $\mu_{1,3}$-azide anions into (4,4) sheets (Figure 2 left). Such a Cu^{II}−N$_3$ (basal-apical coordination) 2-D layered topology is unprecedented, and only a few Ni^{II} and Mn^{II} complexes with similar structures have been reported so far (which is unsurprising given the preference of Ni^{II} or Mn^{II} centers for six-coordination).[13] The bridging **L** ligands then connect these sheets into a single acentric α-Po network (Figure 2 right). Along the [100] direction, the 3-D network shows channels filled by included water molecules, which represents some 24.6% of the total crystal volume (Figure S3). The octahedral Cu^{II} center shows considerable Jahn−Teller distortion (Figure S4), with two of the Cu−N(azide) bonds being considerable longer (2.49(3) and 2.56(3) Å) than the other four Cu−N distances (2.01(2)−2.04(3) Å) as listed in Table 3. The azide ligands bind to Cu^{II} in a nonlinear fashion, with the Cu−N−N angles ranging from 115(2) to 121(2)°.

Table 3. Selected Bond Distances (Å) and Angles (deg) for Complex **2**[a]

Cu(1)−N(8)	2.01(2)	Cu(1)−N(1A)	2.01(2)
Cu(1)−N(5)	2.05(2)	Cu(1)−N(4)	2.04(3)
Cu(1)−N(7B)	2.56(3)	Cu(1)−N(10C)	2.49(2)
N(5)−N(6)	1.16(3)	N(6)−N(7)	1.12(4)
N(8)−N(9)	1.19(3)	N(10)−N(9)	1.20(3)
N(1A)−Cu(1)−N(8)	92(1)	N(8)−Cu(1)−N(5)	176(2)
N(1A)−Cu(1)−N(5)	91(1)	N(8)−Cu(1)−N(4)	88(1)
N(4)−Cu(1)−N(5)	89(1)	N(1A)−Cu(1)−N(4)	177(1)
Cu(1)−N(5)−N(6)	121(2)	Cu(1)−N(8)−N(9)	120(2)
Cu(1)−N(7B)−N(6B)	119(2)	Cu(1)−N(10C)−N(9C)	115(2)
N(5)−N(6)−N(7)	176(4)	N(8)−N(9)−N(10)	174(3)

[a] Symmetry operations: (A) $-x, -y-1, z-1/2$; (B) $x+1/2, -y-1/2, z$; (C) $x-1/2, -y-3/2, z$.

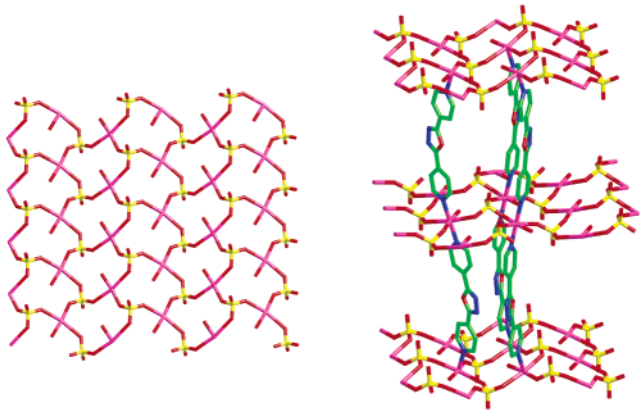

Figure 3. Structure of **3**, showing (left) the bridging of the metal ions by μ_3 bridging sulfate anions into a (6,3) sheet and (right) the bridging of these sheets by **L** into a single chiral 3-D network. Copper atoms are purple, oxygens red, sulfurs yellow, nitrogens blue, and carbons green.

In the structure of complex **3**, the sulfate anions are in μ_3 mode and bridge the Cu^{II} centers into (6,3) networks in which the nodes are alternating Cu^{II} and sulfur atoms (Figure 3, left).[14] These sheets are then connected together by **L** into a chiral 3-D network (Figure 3, right). The topology of this net has the Schäfli symbol $(6^3).(6^9.8)$. A closely related network topology with the same Schäfli symbol is shown by [Ag(C(CN)$_3$)(pyrazine)];[15] however, the two network topologies differ in the relative orientation of the (6,3) sheets. In the crystal structure of **3**, the three five-connecting centers in any six-membered ring with one (6,3) sheet are connected to five-connecting centers belonging to three separate six-membered rings (but connected by a single three-connecting center) in the adjoining (6,3) sheets above and below. In contrast, in [Ag(C(CN)$_3$)(pyrazine)] the equivalent three five-connecting centers are joined to five-connecting centers in

(12) Spek, A. L. *Platon, A Multipurpose Crystallographic Tool*; Utrecht University: Utrecht, The Netherlands, 1999.

(13) (a) Cs$_2$[Ni(N$_3$)$_4$]·H$_2$O: Maier, H. E.; Krischner, H.; Paulus, H. *Z. Kristallogr.* **1981**, *157*, 277−289. (b) [Mn(minc)$_2$(N$_3$)$_2$]$_n$: Escuer, A.; Vicente, R.; Goher, M. A. S.; Mautner, F. A. *J. Chem. Soc., Dalton Trans.* **1997**, 4431−4434. (c) [Mn(4-acpy)$_2$(N$_3$)$_2$]: Escuer, A.; Vicente, R.; Goher, M. A. S.; Mautner, F. A. *Inorg. Chem.* **1995**, *34*, 5707−5708. (d) [Mn(DENA)$_2$(N$_3$)$_2$]: Goher, M. A. S.; Abu-Youssef, M. A. M.; Mautner, F. A.; Vicente, R.; Escuer, A. *Eur. J. Inorg. Chem.* **2000**, 1819−1823.

(14) A similar 2-D structure has been observed in complex [Cu(bpe)(MoO$_4$)], where the anions MoO$_4^{2-}$ bridge the Cu^{II} centers to describe a plane like in compound **2**; see: Hagrman, D.; Haushalter, R. C.; Zubieta, J. *Chem. Mater.* **1998**, *10*, 361−365.

(15) Batten, S. R.; Hoskins, B. F.; Robson, R. *New J. Chem.* **1998**, *22*, 173−175.

Table 4. Selected Bond Distances (Å) and Angles (deg) for Complex **3**[a]

Cu(1)−O(6)	1.995(3)	Cu(1)−N(1)	2.022(3)
Cu(1)−N(2A)	2.045(4)	Cu(1)−O(4B)	2.599(4)
Cu(1)−O(5C)	2.405(3)	Cu(1)−O(2)	1.982(3)
O(2)−Cu(1)−O(6)	172.6(1)	N(1)−Cu(1)−O(2)	89.2(1)
N(1)−Cu(1)−O(6)	89.6(1)	N(2A)−Cu(1)−O(2)	90.3(1)
N(2A)−Cu(1)−O(6)	90.8(1)	N(1)−Cu(1)−N(2)	179.2(2)

[a] Symmetry operations: (A) $-x + 1.5, -y + 1, z - 1/2$; (B) $-x, y, z$; (C) $-x + 2, y - 1/2, -z + 3/2$.

the adjoining (6,3) sheets which are also part of a single six-membered ring. Along the [100] direction, the 3-D network shows chiral channels filled by water molecules which represents ca. 20.0% of the total crystal volume (Figure S5). The coordination environment of Cu^{II} in complex **3** is also an elongated octahedron: as well as three sulfate anions and two ligands **L**, the Cu^{II} atom coordinates to a monodentate water ligand (see Figure S6). The Jahn−Teller distortion is again such that two of the Cu−anion bonds are longer (2.405(3) and 2.599(4) Å) than the other four (1.982(3)−2.045(4) Å) as shown in Table 4.

Removal and Reintroduction of Guest Molecules: TGA and XRPD Studies. The X-ray single-crystal structures of complexes **1**−**3** all contain included water molecules, indicating their porous nature. However, complex **1**, just like **1a**,[6a] is not stable when exposed to air even at room temperature, and X-ray powder diffraction (XRPD) result shows that part of the crystals has become amorphous. It has been well-known that metal−azide complexes containing organic ligands are potentially explosive, and this happens for complex **2** when elevating the temperature to ∼190 °C according to the result of the thermogravimetric analysis (TGA). Complex **3** is stable at room temperature, and the structure indicates that open chiral channels occupied by guest water molecules exist. We were intrigued by the possibility of generating a chiral microporous framework by removing the guest molecules. Thus, we have studied in detail the framework stability and removal−reintroduction of the guest molecules of compound **3**, using TGA and XRPD techniques.

For the TGA curve of **3** (Figure S7), the first weight loss of 8.46% from 75 to 105 °C corresponds to two guest water molecules, and the loss of the coordinated aqua ligand is not observed before 350 °C, where the decomposition starts, maybe due to its strong coordination to Cu^{II} center. Upon evacuation at 180 °C for 6 h, complex **3** experienced weight losses being consistent with the removal of two included water molecules/formula unit. It is interesting that the XRPD pattern for this sample (the calculated XRPD pattern of complex **3** according to the single-crystal diffraction data are shown in Figure S8, being identical to the experimental case) remains essentially identical with that of complex **3**. Moreover, the guest water species can be reintroduced into the evacuated sample of **3** by exposure to water vapor for 12 h, which is confirmed by XRPD (Figure 4), the weight gain of the sample, and elemental analyses. The above results clearly demonstrated that, after removal of the included water molecules, the microporous chiral solid $\{[Cu\mathbf{L}(H_2O)(SO_4)]\}_n$ (**3a**) was generated that retains the framework integrity of the pristine solid **3**. Such a chiral microporous material with high thermal stability (an important precondition in the conversion of the microporous frameworks from laboratory curiosities to practical materials) is quite rare.

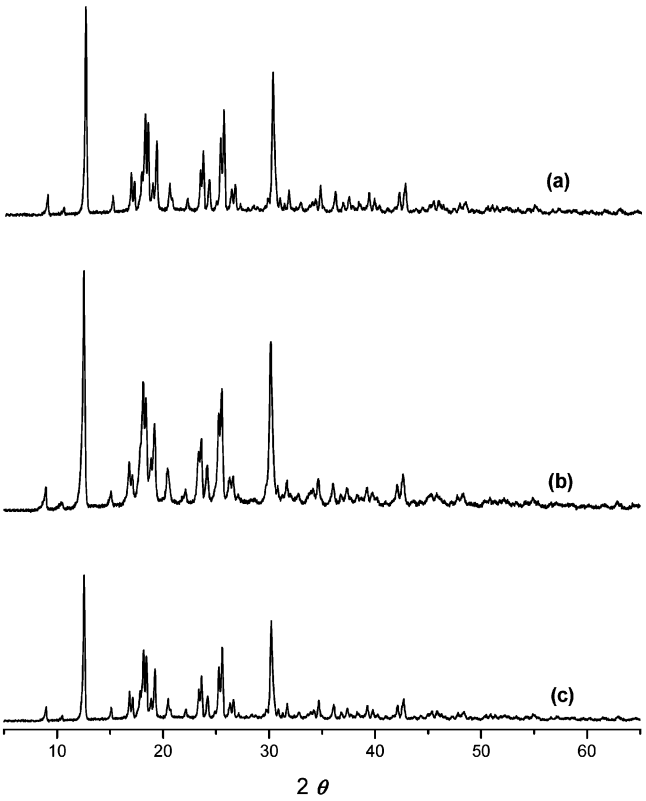

Figure 4. XRPD patterns for **3** (a) taken at room temperature, (b) after removal of the guest water molecules, and (c) after reintroduction of the guest water molecules.

Magnetic Properties. Our previous work has clearly demonstrated that for compound **1a** (in which the Cu^{II} ions are linked only by the long organic fragments **L**) no significant magnetic coupling was observed,[6a] and this is also the case for its isostructural complex **1** reported here.

For complex **2**, the $\chi_M T$ value (χ_M is the molar magnetic susceptibility/Cu^{II} ion) is 0.432 $cm^3\ mol^{-1}$ K at 300 K, corresponding to one spin doublet with $g > 2.00$. Then it decreases monotonically until 2 K, attaining a value of 0.14 $cm^3\ mol^{-1}$ K. This global feature is characteristic of the weak antiferromagnetic interactions between Cu^{II} ions (Figure 5). The χ_M values start from 0.00179 $cm^3\ mol^{-1}$ at 300 K to 0.072 $cm^3\ mol^{-1}$ at 2 K.

To interpret the magnetism of **2**, it is necessary to do some hypothesis, taking into account the structure. This structure is a 3-D network but with a typical feature: it is formed by 2-D coordination layers of Cu^{II} linked only by the azide groups, which are extended by the ligand **L**. The coupling given by the ligand is nil, as we have shown with the magnetic coupling of complexes **1** or **1a**. Thus, from the magnetic point of view, it is obvious that the effective magnetic couplings only exist in the $Cu-N_3$ quadratic 2-D layers, and as indicated above, this represents a new topological type for such system. With focus on this 2-D

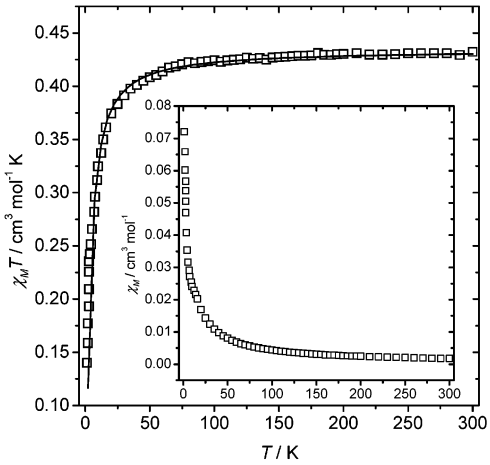

Figure 5. Plots of χ_M (inset) and $\chi_M T$ vs T for complex **2**. Open points represent the experimental values, and the solid line represents the best fit.

sheet, in each Cu_4 entity there are two different azide bridges but both with *end-to-end* coordination, thus giving the antiferromagnetic coupling.[16] All the other structural parameters, such as Cu−N bond lengths (one is short and the other long), Cu−N−N bond angles (∼120°), and Cu−N_3−Cu torsion angles (∼160°), also indicate antiferromagnetic coupling as reported in the literature.[16] From a theoretical point of view, two different J values would be necessary to fit the experimental magnetic data. However, taking into account the similar structural parameters, it is possible to simplify the magnetism considering only one average J value. Thus, we may fit the experimental data with a Lines expression (for quadratic layers with $S = 1/2-5/2$).[17] The exchange Hamiltonian is $H = -\Sigma_{nn} J S_i \cdot S_j$, where Σ_{nn} runs over all pairs of nearest-neighboring spins i and j. The equation is

$$Ng^2\beta^2/\chi|J| = 3\Theta + (\sum C_n/\Theta^{n-1})$$

in which $\Theta = kT/|J|S(S+1)$, N, g, and β have their usual meanings, and, for the $S = 1/2$ system, $C_1 = 4$, $C_2 = 2.667$, $C_3 = 1.185$, $C_4 = 0.149$, $C_5 = -0.191$, and $C_6 = 0.001$. The best fit is as follows: $J = -1.94$ cm^{-1}; $g = 2.15$; $R = 3 \times 10^{-5}$ ($R = \Sigma[(\chi_M T)_{obs} - (\chi_M T)_{calc}]^2/\Sigma[(\chi_M T)_{obs}{}^2]$). To corroborate the order of magnitude of this small antiferromagnetic parameter, magnetizations were measured at 2 K. The reduced magnetization ($M/N\beta$) curve vs H does not follow the Brillouin law (Figure S9). The experimental points are below the Brillouin law curve, indicating weak antiferromagnetism. At 5 T the $M/N\beta$ value tends to 0.32, much more lower than 1, corresponding to an $S = 1/2$ ground state (close to saturation).

For complex **3**, the $\chi_M T$ value (χ_M is the molar magnetic susceptibility/Cu^{II} ion) is 0.465 cm^3 mol^{-1} K at 300 K, corresponding to one independent Cu^{II} ion without coupling ($g > 2.00$); it is almost constant to 20 K and, finally, increases slightly with further cooling, attaining a maximum

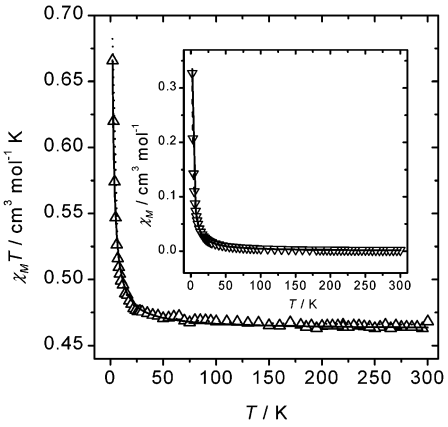

Figure 6. Plots of χ_M (inset) and $\chi_M T$ vs T for complex **3**. Open points represent the experimental values and solid lines the best fit (see text for the two models).

of 0.67 cm^3 mol^{-1} K at 2 K (Figure 6). This feature is characteristic of the presence of very small ferromagnetic coupling between Cu^{II} ions. Considering once again such as in complexes **1** and **2** that **L** does not create any magnetic coupling, two approaches have been made to fit the magnetic data. The first assumes a trigonal layer in which each Cu^{II} ion is linked by μ-SO_4 bridging ligands to other copper ions, with only one J parameter (a little bit unrealistic; see below). Thus, we fitted the experimental data with the de Jongh expression (for a ferromagnetic trigonal layer with $S = 1/2$).[18] The exchange Hamiltonian is $H = -\Sigma_{nn} J S_i \cdot S_j$, where Σ_{nn} runs over all pairs of nearest-neighboring spins i and j. The equation is

$$(Ng^2\beta^2/4k)F$$

N, g, β, and k have their usual meanings and $F = 1 + \Sigma(A_n K^n)$ [$K = J/kT$; the coefficients for n are +3 ($n = 1$), +6 ($n = 2$), +8.5 ($n = 3$), +9.375 ($n = 4$), +11.025 ($n = 5$), +16.964 583 333 ($n = 6$), +21.152 678 571 ($n = 7$), +8.805 877 976 2 ($n = 8$), and −9.678 455 687 8 ($n = 9$), respectively]. The best fit is as follows: $J = +0.17$ cm^{-1}; $g = 2.21$; $R = 2 \times 10^{-5}$ ($R = \Sigma[(\chi_M T)_{obs} - (\chi_M T)_{calc}]^2/\Sigma[(\chi_M T)_{obs}{}^2]$). The second approach has been made by assuming that the actual structure, from a magnetic point of view, is uniform one-dimensional, because the longest Cu−OSO_3 is 2.6 Å. The formula given by Baker et al. for a ferromagnetic one-dimensional $S = 1/2$ chain is only a high-temperature series expansion,[19] thus, not very accurate for complex **3**, in which the ferromagnetic character is undoubtely very small. For this reason we decided to do a full diagonalization of the system through the Clumag program,[20] using 12 cycled Cu^{II} ions that allow close representation of the infinite character of the chain. The best fit is as follows: $J = +0.43$ cm^{-1}; $g = 2.22$; $R = 1 \times 10^{-4}$ ($R = \Sigma[(\chi_M T)_{obs}$

(16) (a) Comarmond, J.; Plumere, P.; Lehn, J.-M.; Agnus, Y.; Louis, R.; Weiss, R.; Kahn, O.; Morgenstern-Badarau,I. *J. Am. Chem. Soc.* **1982**, *104*, 6330−6340. (b) Thompson, L. K.; Tandon, S. S. *Comments Inorg. Chem.* **1996**, *18*, 125−144.
(17) Lines, M. E. *J. Phys. Chem. Solids* **1970**, *31*, 101−106.
(18) De Jongh, L. J. In *Magnetic Properties of Layered Transition Metal Compounds*; Navarro, R., Ed.; Kluwer Academic Publishers: Dordrecht, The Netherlands, 1990; Vol. 9, pp 105−190.
(19) Baker, G. A.; Rushbrooke, G. S.; Gilbert, H. E. *Phys. Rev. A* **1964**, *135*, 1272.
(20) The series of calculations were made using the computer program CLUMAG, which uses the irreducible tensor operator (ITO) formalism: Gatteschi, D.; Pardi, L. *Gazz. Chim. Ital.* **1993**, *123*, 231.

$- (\chi_M T)_{calc}]^2/\Sigma[(\chi_M T)_{obs}{}^2]$). Thus, in both cases (fitting as a trigonal two-dimensional layer or as a one-dimensional uniform chain), the *J* value is very small and ferromagnetic. If one looks at the structure, the Cu^{II} ions are linked by SO_4^{2-} anions in an axial−equatorial form, which may result in very small ferromagnetic coupling. Indeed, although the number of (μ-sulfato)copper(II) complexes is large, those with only a μ-SO_4 bridging ligand and magnetic data are very reduced. In fact, to the best of our knowledge, only two complexes have been magnetically studied: the first one is $[Cu(oaoH_2)(H_2O)(SO_4)]_2$, for which a *J* value of -1.27 cm^{-1} has been reported.[21] In this complex, according to the authors, important hydrogen bonds between water molecules and sulfate anions are present. The second one is $[Cu(PAHOX)(SO_4)]\cdot 2H_2O$, for which the authors state "this complex is completely uncoupled, consistent with the axial−equatorial arrangement of bonds to the sulfate bridges, leading to effective orthogonality between the copper magnetic orbital".[22] We believe that this orthogonality could also give a small ferromagnetic coupling, as observed in complex **3**. For the reduced magnetization ($M/N\beta$) vs *H* curve (Figure S10), the experimental points (at 2 K) follow the Brilloiun formula for an $S = 1/2$ system with $g = 2.2$. This feature clearly indicates that the ferromagnetic coupling is very small.

(21) Endres, H.; Nothe, D.; Rossato, E.; Hatfield, W. E. *Inorg. Chem.* **1984**, *23*, 3467.

(22) Thompson, L. K.; Xu, Z.; Goeta, A. E.; Howard, J. A. K.; Clase, H. J.; Miller, D. O. *Inorg. Chem.* **1998**, *37*, 3217.

Conclusion and Comments

In summary, two unique acentric solids based on 3-D metal−organic coordination networks have been prepared through an anion-exchange procedure and the corresponding porous and magnetic properties have been investigated. This study also clearly indicates that the coordination ability of the counteranions can play an important role in crystal engineering (especially for acentric coordination polymers in this work) and suggests that given the simple permutations of the anions, Cu^{II} alone might have a rich and diverse role in construction of coordination frameworks. Of further interest, we can expect that using larger anions or a bulky substituent on one of the pyridine rings may also prevent interpenetration and create other novel chiral porous materials with large chiral voids, which is now under investigation in our laboratory.

Acknowledgment. This work was financially supported by the Outstanding Youth Foundation of the NSFC (No. 20225101) and the Spanish government (Grant BQU2000-0791).

Supporting Information Available: Three X-ray crystallographic files in CIF format for complexes **1**−**3**, an illustration of the coordination environment of the Cu^{II} center in complexes **1**−**3**, a TGA curve and simulated XRPD pattern of compound **3**, and magnetization measurements for complexes **2** and **3**. This material is available free of charge via the Internet at http://pubs.acs.org.

IC0351242